JOURNAL OF SOLID STATE CHEMISTRY 99, 110–119 (1992)

Synthesis, Structure Determination, and Ionic Conductivity of Sodium Tetrathiophosphate

M. JANSEN* AND U. HENSELER

Institut für Anorganische Chemie der Universität Bonn, Gerhard-Domagk-Str. 1, W-5300 Bonn 1, Germany

Received October 8, 1991; in revised form December 30, 1991; accepted January 9, 1992

Single-phase colorless sodium thiophosphate powders and transparent colorless single crystals of the low-temperature phase of Na_3PS_4 have been synthesized by solid-state reaction from sodium metal, sulfur, and tetraphosphorusdecasulphide. At 261°C a phase transition from α- to β-Na_3PS_4 has been established via differential thermal analysis and temperature-dependent X-ray powder diffraction. X-ray structure analysis has been performed for the low-temperature phase at 25°C. The space group is $P\bar{4}2_1c$, with $a = 695.20(4)$ pm and $c = 707.57(5)$ pm. The compound consists of sodium cations and isolated PS_4^{3-} anions with two formula units per unit cell. AC-conductivity measurements show Na_3PS_4 to be a good ionic conductor with conductivities between $\sigma = 4.17 \times 10^{-6}\ \Omega^{-1}\ cm^{-1}$ (at 50°C) and $\sigma = 8.51 \times 10^{-2}\ \Omega^{-1}\ cm^{-1}$ (at 510°C). The activation energies for ion transport are 40.1 kJ mole^{-1} for α-Na_3PS_4 and 38.8 kJ mole^{-1} for β-Na_3PS_4. Above 490°C there is evidence for a second high-temperature phase existing with dynamically disordered anions, causing a steep increase in conductivity.

Introduction

Most salts containing complex anions undergo at least one structural phase transition which is accompanied by a sharp increase of rotational diffusion of the anions. There has been some controversy as to whether the rotationally mobile but translationally fixed anions allow for better cation conductivity (*1*). In some reports evidence for this "cogwheel" or "paddle wheel" effect has been claimed (*2–4*); others try to explain the experimental results by a "volume effect" (*5–7*). A good candidate to contribute to a solution of this mechanistic problem might be sodium tetrathiophosphate. Although syntheses and crystal structures of Li_3PS_4 and K_3PS_4 have been well established (*8*, *9*), Na_3PS_4 has not been prepared in a pure state, so far, and its crystal structure is still unknown.

At establishing the phase diagram of the system Na_2S/P_4S_{10}, a phase transition from α- to β-Na_3PS_4 has been detected (*10*). Besides, the vibrational spectra of Na_3PS_4 have been recorded (*11*, *12*).

Experimental

Synthesis. Na_3PS_4 was synthesized by solid-state reaction via two different routes. Single-phase, colorless sodium thiophosphate powders were obtained by reaction of purified sodium metal (liquation refining) with an appropriate mixture of purified sulfur (liquid sulfur chromatographed through

* To whom correspondence should be addressed.

0022-4596/92 $5.00

MgO and α-Al_2O_3) and tetraphosphorusdecasulfide (recrystallized from CS_2) in a glass ampoule sealed under vacuum. Because of the strong exothermal character of the reaction between the starting materials at direct contact, sodium was separated from the mixture of sulfur and phosphorussulfide in order to allow for reaction only via the vapor phase. A heating rate of 20°C/hr, a final reaction temperature of 350°C, and a reaction time of 7 days proved to be the best parameters. The inhomogenous raw product was finely ground in an agate mortar (glove box) and heated again in a silica ampoule, sealed under vacuum, to a final temperature of 750°C. The heating rate was 250°C/hr, the reaction time at 750°C was 1 hr, and the cooling rate was 50°C/hr. The obtained product was identified by X-ray powder diffraction (Stoe-Stadi P diffractometer with position sensitive detector, germanium monochromator and Cu$K\alpha$-radiation (λ = 154.056 pm)), and infrared spectroscopy (Bruker IFS 113v, scan range 150–4000 cm^{-1}, CsI disks). Both methods confirmed the absence of impurities.

Single crystals of α-Na_3PS_4 were prepared by reacting appropriate proportions of disodiummonosulphide (made from sodium and sulfur by solid-state reaction) and tetraphosphorusdecasulphide in the solid state. For this purpose, the finely ground mixture was heated in a silica ampoule sealed under vacuum at a rate of 50°C/hr to 550°C, cooled down to 500°C at 10°C/hr, held at this temperature for 12 hr, and finally cooled down to room temperature at 20°C/hr. Colorless, transparent single crystals thus were obtained.

Handling of substances and preparations were invariably carried out in an atmosphere of very dry argon due to the sensitivity of the starting materials and the product to air and moisture.

Structure determination. For data collection one crystal (approximately 0.12 mm in diameter) was sealed under argon in a Lindemann-capillary. Lattice parameters were determined by least-squares refinement of 25 reflections with high indices. Intensity measurements were carried out on an Enraf-Nonius CAD4 automatic four circle diffractometer equipped with a graphite monochromator and Mo$K\alpha$-radiation (λ = 71.069 pm).

Crystal data and experimental details of the data collection are listed in Table I. Lorentz and polarization corrections were applied to the data. Because of their higher accuracy, the cell parameters obtained from the powder pattern by indexing and least-squares refinement (Stoe-Stadi P software) were used in all further calculations (c.f. Table II).

TABLE I

EXPERIMENTAL DETAILS OF THE STRUCTURE DETERMINATION FOR α-Na_3PS_4

Molecular weight [g mol^{-1}]	228.2
Space group	$P\bar{4}2_1c$ (No. 114)
Cell dimensions [pm]	a = 695.20(4)
(refined from powder pattern)	c = 707.57(5)
Cell volume [10^6 pm^3]	341.97(4)
D_{calc} [g cm^{-3}]	2.22
Θ range for data collection [°]	$1 \leq \Theta \leq 35$
h,k,l range for data collection	−11,11; −11,11; −12,12
Scan mode	ω/Θ
Scan width [°]	0.55 + 0.35 tan Θ
Max. scan time [sec]	120
F (000)	223.95
μ [cm^{-1}]	15.52
No. of reflections measured	6318
No. of unique reflections	751
Internal R-value [%]	2.2
No of reflections with $F_o > 2\sigma(F_o)$ used for final refinement	745
No. of parameters	19
R-value [%]	4.20
wR-value [%]	3.93
Weight	$3.23/\sigma^2(F)$
Maximum shift/e.s.d.	0.004
Maximum height in difference fourier map [e pm^{-3}]	1.25×10^{-6}

TABLE II

X-RAY PATTERN OF α-Na_3PS_4: MILLER INDEX, RELATIVE INTENSITIES, OBSERVED, d_o [Å], AND CALCULATED, d_c [Å], SPACINGS

hkl	I/I_{max}	d_o	d_c	*hkl*	I/I_{max}	d_o	d_c
101	47.4	4.9571	4.9590	411	17.9	1.6398	1.6402
110	14.1	4.9129	4.9158	330			1.6386
200	4.8	3.4761	3.4760	204	3.6	1.5763	1.5765
102	3.7	3.1541	3.1531	402	6.6	1.5598	1.5599
201	3.8	3.1152	3.1198	420	10.9	1.5544	1.5545
112	49.1	2.8710	2.8715	421	1.2	1.5187	1.5183
211	100.0	2.8463	2.8464	323	2.3	1.4929	1.4928
202	52.9	2.4792	2.4795	332	0.6	1.4868	1.4869
220	37.2	2.4579	2.4579	224	2.4	1.4357	1.4358
212	13.9	2.3358	2.3354	422	8.1	1.4231	1.4232
103	7.1	2.2334	2.2335	314	4.6	1.3782	1.3782
301	15.1	2.2004	2.2022	431	3.3	1.3641	1.3643
310			2.1984	510			1.3634
311	1.6	2.0999	2.0994	324	1.2	1.3034	1.3035
222	23.2	2.0186	2.0186	432	3.5	1.2942	1.2940
213	5.5	1.8787	1.8791	215	2.9	1.2879	1.2880
312	9.1	1.8671	1.8673				
321	6.8	1.8603	1.8603				
400	1.1	1.7378	1.7380				
104	1.5	1.7149	1.7143				
114	6.8	1.6647	1.6644				
303	14.4	1.6530	1.6530				

All calculations[1] were performed with a micro VAX II computer using the programs SHELXS-86 (*13*) for data reduction and structure solution by direct methods and SHELX-76 (*14*) for final refinement by full-matrix least-square methods. The final residuals are shown in Table I. Structure plots were generated using the programs KPLOT (*15*) and ORTEP (*16*).

Thermal analysis. Differential thermal analysis (DTA) combined with thermogravimetry (TG) was performed with a Netsch STA 429 using the following operating parameters: sensitivity TG: 125 mg, DTA: 100 μV, DTG: 100 μV; speeds of heating and cooling: 5°C/min; corundum container; argon atmosphere; reference: high-purity Al_2O_3.

Temperature-dependent powder X-ray diffraction patterns were recorded using an Enraf-Nonius high-temperature Guinier-camera FR 553.

Ionic conductivity measurements. The electrical conductivity of Na_3PS_4 was determined by impedance spectroscopy in the frequency range 5 Hz–13 MHz with blocking platinum electrodes using compact polycrystalline powder samples (diameter: 9 mm, thickness: 1–2 mm; pressed with 780 MPa, sintered at 480°C for 1 hr). The samples were contacted by pressing silver foil (thickness: 0.125 mm) onto the pellet coated

[1] Further details of the structure determination have been deposited as Supplementary Publication No. CSD-55734. Copies may be obtained through Fachinformationszentrum Karlsruhe, Gesellschaft für wissenschaftlich technische Information mbH, W-7514 Eggenstein-Leopoldshafen 2, Germany.

TABLE III

FRACTIONAL COORDINATES AND ANISOTROPIC TEMPERATURE FACTORS FOR α-Na_3PS_4

Atom	Wyckoff notation	Atomic parameters x	y	z
Na(1)	4*d*	0	0.5	0.42066(36)
Na(2)	2*a*	0	0	0
P	2*b*	0	0	0.5
S	8*e*	0.31244(12)	0.34755(12)	0.16502(13)

Atom	Thermal parameters[a] U_{11}	U_{22}	U_{33}	U_{12}	U_{13}	U_{23}
Na(1)	0.0416(15)	0.0188(11)	0.0474(14)	−0.0035(10)	0	0
Na(2)	0.0693(19)	0.0693(19)	0.0232(17)	0	0	0
P	0.0125(4)	0.0125(4)	0.0141(6)	0	0	0
S	0.0214(4)	0.0168(3)	0.0210(3)	0.0027(4)	0.0081(3)	−0.0005(3)

[a] The general temperature factor expression of an atom for a given set of planes (*hkl*) is $\exp[-2\pi^2(U_{11}h^2a^{*2} + U_{22}k^2b^{*2} + U_{33}l^2c^{*2} + 2U_{13}hla^*c^*\ \mathrm{H} + \ldots)]$, where the U_{ij} are the thermal parameters expressed in terms of the mean-square amplitudes of vibration in angstroms.

with graphite, yielding a sandwich Ag/$C_{graph.}$/Na_3PS_4/$C_{graph.}$/Ag.

The AC-conductivity was measured in a glass cell described elsewhere (*17*) under dry argon using a computer controlled impedance bridge (Hewlett–Packard 4192A LF). Conductivity data were collected as a function of temperature in the range from 50 to 550°C with a heating and cooling rate of 20°C/hr. Determination of the electronic part of conductivity was carried out by dc-measurements in the range 50–350°C in steps of 50°C using the same samples as in the ac-experiments.

Results and Discussion

Crystal structure. Fractional coordinates and anisotropic temperature factors of α-Na_3PS_4 are given in Table III. Selected bond distances and angles are reported in Table IV.

The low-temperature form of Na_3PS_4 crystallizes tetragonally in the space group

TABLE IV

IMPORTANT BOND DISTANCES AND ANGLES IN α-Na_3PS_4

	Bond distance [pm]		
About Na(1)		About Na(2)	
Na(1)–$S^{a,b}$	301.86(21)	Na(2)–$S^{b,c,k,l}$	290.51(17)
–$S^{c,f}$	281.16(16)	–$S^{a,h,i,j}$	345.23(15)
–$S^{d,h}$	297.15(21)		
About P			
P –$S^{b,c,d,e}$	204.61(11)		
	Bond angles [°]		
About P			
S^b–P–S^c	110.42(6)		
–$S^{d,e}$	109.00(5)		
S^c–P–$S^{d,e}$	109.00(5)		
S^d–P–S^e	110.42(6)		

[a] *x*, *y*, *z*; [b] $-x + 0.5$, $y - 0.5$, $-z + 0.5$; [c] $x - 0.5$, $-y + 0.5$, $-z + 0.5$; [d] $-y + 0.5$, $-x + 0.5$, $z + 0.5$; [e] $y - 0.5$, $x - 0.5$, $z + 0.5$; [f] $-x + 0.5$, $y + 0.5$, $-z + 0.5$; [g] $y - 0.5$, $x + 0.5$, $z + 0.5$; [h] $-x$, $-y$, *z*; [i] *y*, $-x$, $-z$; [j] $-y$, *x*, $-z$; [k] $-y + 0.5$, $-x + 0.5$, $z - 0.5$; [l] $y - 0.5$, $x - 0.5$, $z - 0.5$.

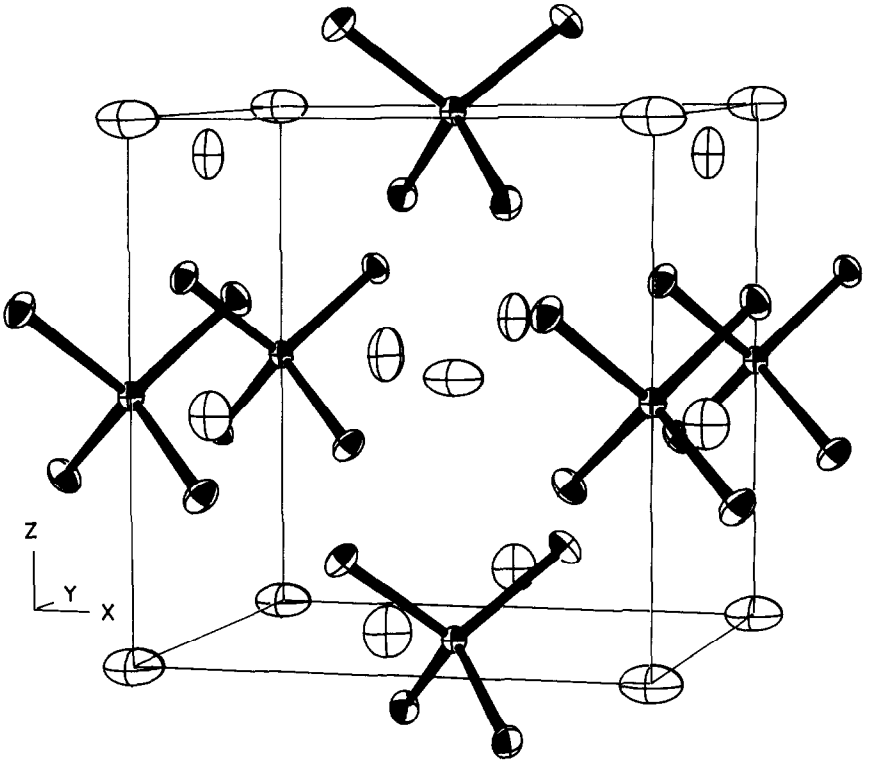

FIG. 1. A view of the unit cell of α-Na_3PS_4.

$P\bar{4}2_1c$ (No. 114) with two formula units per unit cell, and represents a new type of structure for solids of the general formula A_3MX_4. A plot of the structure is given in Fig. 1. Relations to known structures can be drawn by applying to the unit cell the transformation (1,1,0/1,$\bar{1}$,0/0,0,1): an arrangement of the baricenters of the anions in the sense of a cubic closed packing (heavily distorted, however) becomes apparent (c.f. Fig. 2). Just this feature (with cubic symmetry) is present in high-temperature Na_3PO_4 (*18*).

The anion itself exhibits the geometry of a slightly distorted tetrahedron (site symmetry of phosphorus is S_4). The bond length between phosphorus and sulfur is 204.61 pm (4×) which, as expected, lies between the bond length of 191 pm to a terminal sulfur atom and 210 pm to a bridging sulfur atom in P_4S_{10} (*19*). Deviations from the ideal tetrahedral geometry are expressed by the S–P–S bond angles of 110.42° (2×) and 109.00° (4×).

In contrast to this case the PS_4^{3-}-ions in the lithium and potassium compound (*8, 9*) show larger distortions with bond lengths varying between 202 and 208 pm and bond angles between 106° and 113°.

The two crystallographically independent sodium ions show quite different coordinations by sulfur. The sodium ions on the special site 4*c* are surrounded by six sulfur atoms forming a strongly distorted trigonal antiprism (Fig. 3). The sodium–sulfur distances range within 281 to 302 pm. The sodium ions on the special site 2*a* are coordinated eightfold by a strongly distorted cube of sulfur atoms (two bisphenoids penetrat-

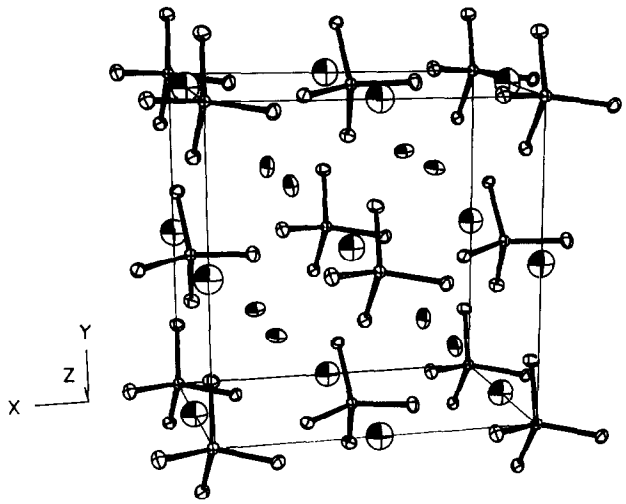

FIG. 2. A view of the transformed unit cell of α-Na_3PS_4, showing the cubic closed-like packing of the PS_4^{3-} ions.

ing each other) (Fig. 3). The sodium–sulfur distances range from 290.51 pm (4×) to 345.23 pm (4×).

Looking at a larger section of the structure (Fig. 4) one realizes rows of isolated thiophosphate tetrahedrons running in three directions orthogonal to each other. The cavities within this array are occupied by linear or zigzag rows of sodium ions. Considering this arrangement and taking into account the somewhat large temperature factors of the sodium ions (Table III), a high and isotropic mobility of the cations in Na_3PS_4 might be expected.

Electrical properties. In order to determine the ionic conductivity impedance measurements at constant temperatures have been performed. A typical result is shown in Fig. 5, where the imaginary part of ac-conductivity is plotted versus its real part (Argand-diagram). From the shape of the curve, conclusions about the different ohmic and capacitive parts of conductivity can be drawn. All measurements at different, but constant, temperatures show one semicircle at the higher frequencies and a linear spike with a nearly 45° incline in the lower frequent part. While the semicircle is caused by the bulk resistance and capacitance of the sample, the spike can be interpreted as a double-layer capacitance according to the blocking electrodes.

The real part of the ac-conductivity corresponding to the minimum imaginary conductivity at lower frequencies was taken as bulk ionic conductivity. The temperature dependence has been determined from 50 to 550°C and plotted in an Arrhenius type of diagram (Fig. 6).

By temperature-dependent powder diffraction and differential thermal analysis a structural phase transition with only a small enthalpy effect has been detected at 261 ± 6°C, which does not seem to be associated with an increase in rotational disorder of the PS_4^{3-}-anion. A second effect below the melting point (517°C) appears between 490 and 510°C, which is accompanied by an endothermic effect almost as strong as at melting (c.f. Fig. 7).

The phase transitions present themselves in the electric behavior, too. Below 261°C,

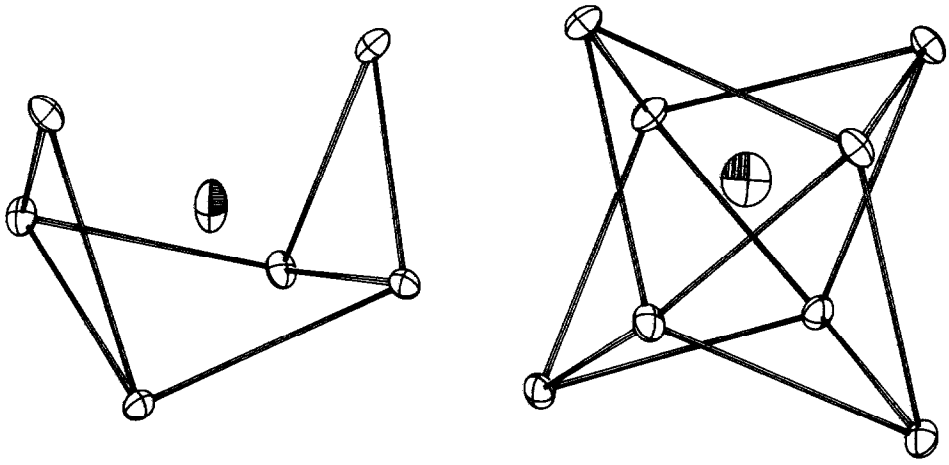

FIG. 3. The sixfold (on the left) and the eightfold (on the right) coordination of sodium cations by sulfur in α-Na_3PS_4.

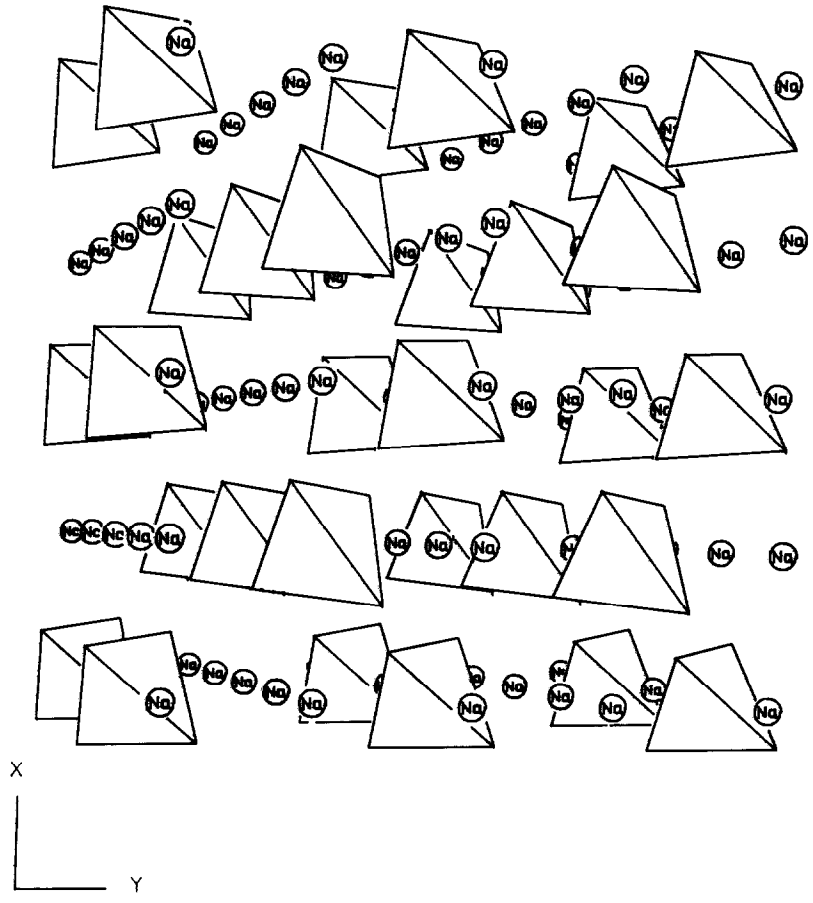

FIG. 4. Extended structure plot of α-Na_3PS_4, showing the sodium ion distribution between the rows of PS_4^{3-} ions (drawn as tetrahedrons) down the z axis.

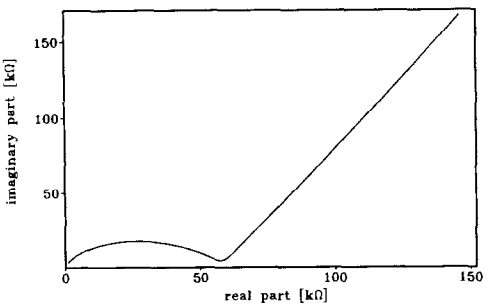

FIG. 5. Argand diagram at 22°C showing the conductivity behavior of Na_3PS_4.

which is the transformation temperature from α- to β-Na_3PS_4, the conductivity and activation energy are calculated to be $\sigma = 7.71 \times 10^{-4}\ \Omega^{-1}\ cm^{-1}$ (at 250°C) and $E_a = 40.1$ kJ mol^{-1} (slope between 50 and 250°C), respectively. The transition, which seems to be predominantly of higher order, is accompanied by only small changes in the electrical characteristics. This is supported by a close relationship of the structures of α- and β-Na_3PS_4, as deduced from comparison of their powder diagrams, by a virtually absent DTA signal and by the X-ray powder lines converging sluggishly. By these observations, an induction period preceeding the transition is indicated. In the stability range of β-Na_3PS_4 the conductivity is $\sigma = 1.55 \times 10^{-2}\ \Omega^{-1}\ cm^{-1}$ (at 450°C) and the activation energy $E_a = 38.8$ kJ mol^{-1} (slope between 294 and 416°C).

In the temperature range of 490 to 510°C, a steep increase in conductivity associated with a strong endothermic effect might be indicative for the onset of rotational motion of the anions. However, attempts to characterize the structural features of this transition have failed because of reactions of Na_3PS_4 with the quartz or glass capillaries. The conductivity data for this second high-temperature phase which we suppose to contain dynamically disordered anions are $\sigma = 8.51 \times 10^{-2}\ \Omega^{-1}\ cm^{-1}$ (at 510°C); above

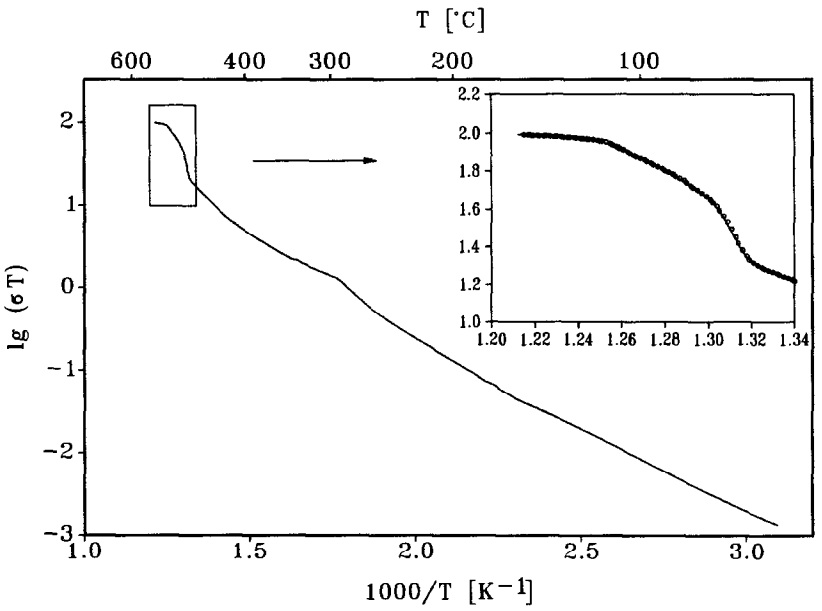

FIG. 6. Arrhenius plot of Na_3PS_4 in the temperature range from 50 to 550°C. The range between 474 and 550°C has been drawn on a larger scale, besides appending the data points (○) to show more details.

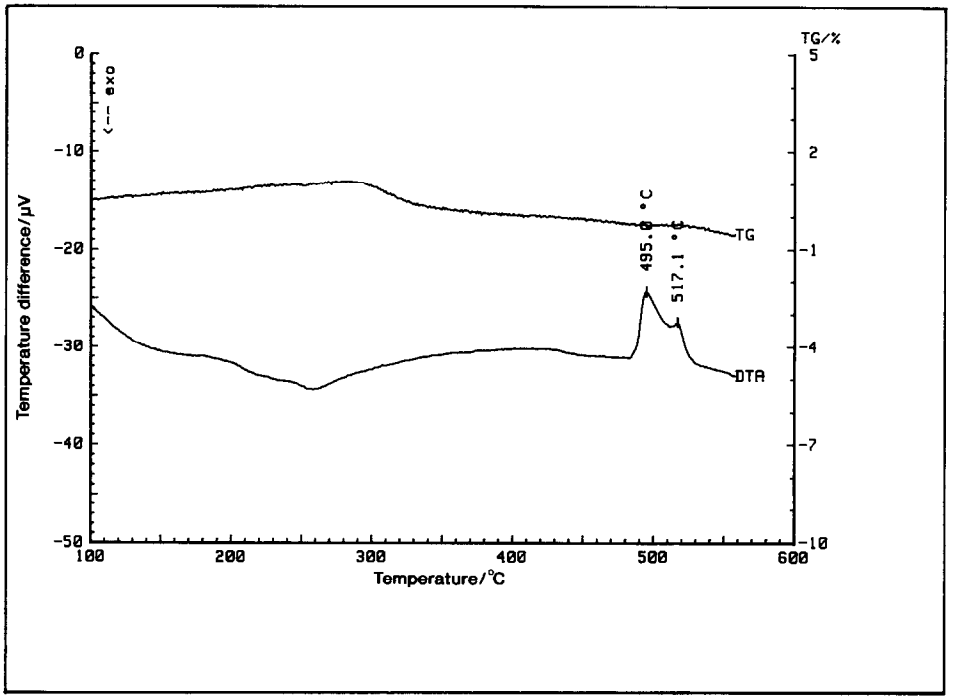

FIG. 7. TGA and DTA traces for Na_3PS_4 (heating cycle).

the melting point $\sigma = 1.03 \times 10^{-1}\,\Omega^{-1}\,cm^{-1}$ and an activation energy $E_a = 13.5\,kJ\,mol^{-1}$ (slope between 522 and 550°C) have been determined. It should be mentioned that the mechanical stability was good up to the melting point, and still satisfactory above 517°C.

As compared to the ionic conductivities of Na_3PO_4 (*20*) ($\sigma = 7.27 \times 10^{-6}\,\Omega^{-1}\,cm^{-1}$ at 250°C, $\sigma = 2.48 \times 10^{-3}\,\Omega^{-1}\,cm^{-1}$ at 450°C, and $\sigma = 4.19 \times 10^{-3}\,\Omega^{-1}\,cm^{-1}$ at 510°C), those of Na_3PS_4 are 6 to 10 times higher concerning the high-temperature phases and 100 times higher regarding the low-temperature phases.

Conclusions

Na_3PS_4 has been synthesized via two different solid-state routes yielding colorless, coarse crystalline samples. It exhibits a singular crystal structure and undergoes two phase transitions in the solid state. Measurements of the ionic conductivity and DTA experiments indicate premelting effects about 30°C below the melting point.

Acknowledgment

We thank the Deutsche Forschungsgemeinschaft for the financial support.

References

1. M. JANSEN, *Angew. Chem.*, **103,** 1574 (1991); *Angew. Chem. Int. Ed. Engl.* **30,** 1547 (1991).
2. A. LUNDÉN, *Solid State Commun.* **65,** 1237 (1988).
3. A. LUNDÉN, *Solid State Ionics* **28–30,** 163 (1988).
4. A. LUNDÉN, AND M. A. K. L. DISSANAYAKE, *J. Solid State Chem.* **90,** 179 (1991).
5. E. A. SECCO, *Solid State Commun.* **66,** 921 (1988).
6. E. A. SECCO, *Solid State Ionics* **28–30,** 168 (1988).
7. A. S. CAMPELL, K. G. MACDONALD, AND E. A. SECCO, *J. Solid State Chem.* **81,** 65 (1989).
8. R. MERCIER, J.-P. MALUGANI, B. FAHYS, AND G. ROBERT, *Acta Crystallogr. Sect. B* **38,** 1887 (1982).

9. H. SCHÄFER, G, SCHÄFER, AND A. WEISS, *Z. Naturforsch. B: Anorg. Chem. Org. Chem.* **20,** 811 (1965).
10. R. BLACHNIK AND U. RABE, *Z. Anorg. Allg. Chem.* **462,** 199 (1980).
11. W. BROCKNER, private communication.
12. M. M. MAURICE, J. F. LEROY, G. KAUFMANN, A. MÜLLER, AND H. W. ROESKY, *C. R. Acad. Sci. Paris Ser. C* **267,** 563 (1968).
13. G. M. SHELDRICK, "SHELXS-86 Program for Crystal Structure Solution," Universität Göttingen, Germany (1986).
14. G. M. SHELDRICK, "SHELX-76 Program for Crystal Structure Determination," University of Cambridge, England (1976).
15. R. HUNDT, "KPLOT Program for Plotting and Investigating Crystal Structures," Universität Bonn, Germany (1979).
16. C. K. JOHNSON, "ORTEP Program for Plotting Crystal Structures on a Plotter," Oak Ridge National Laboratory, TN (1970).
17. U. KÖHLER AND M. JANSEN, Thesis, U. Köhler, Universität Hannover (1987).
18. D. M. WIENCH AND M. JANSEN, *Z. Anorg. Allg. Chem.* **461,** 101 (1980).
19. A. VOS, R. OLTHOF, F. VAN BOLHUIS, AND R. BOTTERWEG, *Acta Crystallogr.* **19,** 864 (1965).
20. H. HRUSCHKA, E. LISSEL, AND M. JANSEN, *Solid State Ionics* **28–30,** 159 (1988).